

I. INTRODUCTION

- Systemic therapy with large-field radiotherapy (RT) to the chest wall and lymph nodes in the mediastinum and axilla yields a substantial survival benefit,¹ but can result in inadvertent exposure of large volumes of normal tissues to low and moderate doses of radiation.
- There is a 7% increase in the relative risk of cardiac events with each 1-Gy increment in mean heart dose, for a 27% total increased relative risk for the typical patient.²
- Left-sided breast cancer patients who receive RT to the chest wall have a 4-fold higher lifetime risk of cardiac events than patients with right-sided breast cancer who receive RT to the chest wall.³
- Because cardiac injury is a known risk of treatment, early markers of heart injury could be beneficial for follow-up management in these patients and may help identify new techniques that would improve the therapeutic ratio of treatment.

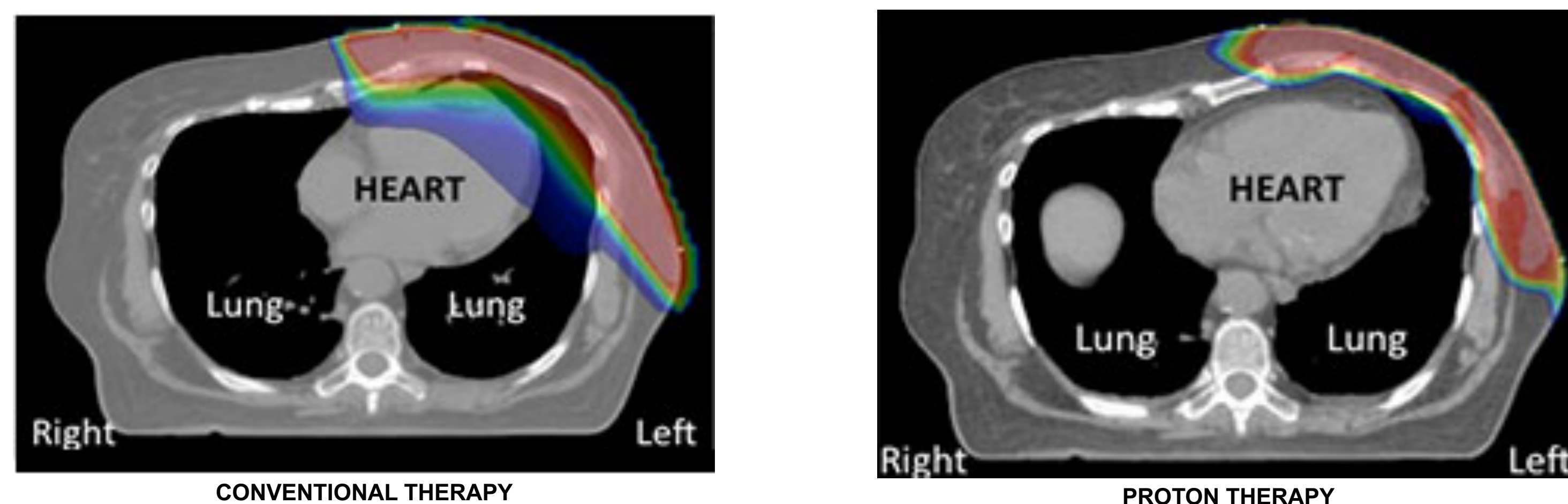


Figure 1: Treatment Plans for Photon vs Proton Therapy: Shown on the left is a conventional X-ray-based radiation treatment plan for a representative left-sided breast cancer patient. The color range from purple to yellow represents low to high radiation exposure. Shown on the right is a proton therapy plan for the same patient using similar constraints for target dose and dose to the heart and other organs at risk.

OBJECTIVE : To quantify subclinical changes in heart function and regional myocardial strains using cardiac magnetic resonance (CMR) images with cardiac tagging to compare risk of cardiac toxicity for standard X-ray based RT versus proton therapy treatment in breast cancer patients.

II. METHODOLOGY

IMAGE ACQUISITION

- CMR images were acquired at 8 to 10 time-frames over the systolic phase of the cardiac cycle in patients with left-sided breast cancer. Eight to 10 short- and long-axis views were acquired before and 6-12 months after completion of RT. Contrast-enhanced images were obtained to assess left ventricular volume and ejection fraction (LVEF). CMR images with parallel tags were acquired for wall strain analysis.

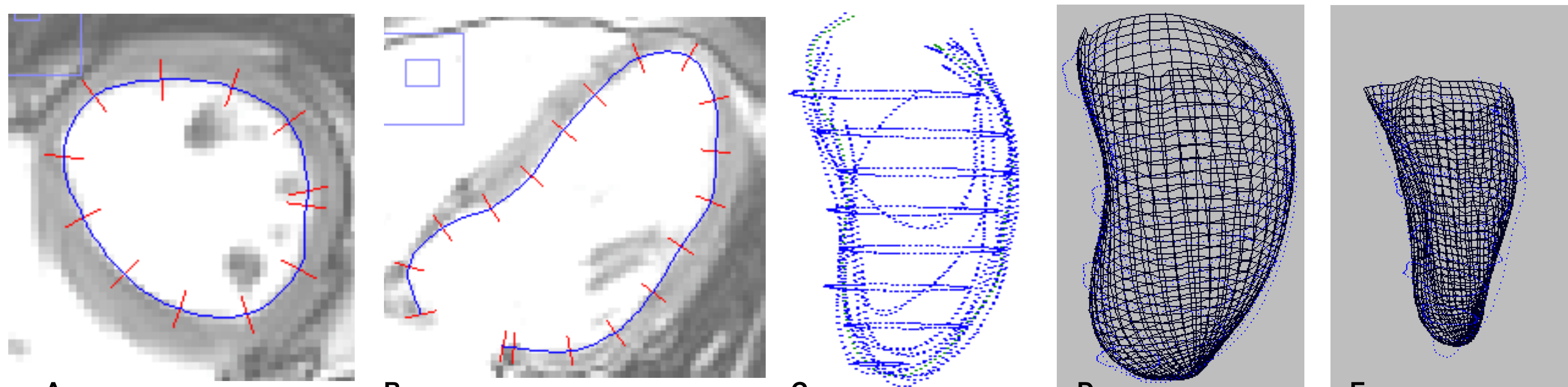


Figure 2. Cardiac MR Images, contour segmentation, and surface fitting: [A] and [B] show representative short- and long-axis CMR images with vascular contrast, overlaid with snake-based endocardial contours. [C] shows the contour points from all slices and views at time 0 (end-diastole). [D] and [E] show endocardial surface meshes generated from the surface models at end-diastole and end-systole, respectively, in the same patient and at same size scale.

HEART LEFT VENTRICLE CONTOUR SEGMENTATION AND CAVITY VOLUME CALCULATION

- An in-house semi-automatic snake based contouring toolkit was used to segment the left ventricular endocardial and epicardial borders on each image slice and time frame (Fig. 2A-C). Mathematical models for each surface were defined in a prolate spheroidal coordinate system with λ , the radial coordinate, expressed as a series expansion in θ and μ , the circumferential and longitudinal angles (Fig. 2D,E).
- Care was taken to demark the mitral valve ring as the first and last contour points in each long-axis view (Fig. 2B).

DEFORMABLE IMAGE REGISTRATION AND STRAIN CALCULATIONS

- The motion of the heart was modeled by modes of deformation defined in the local heart-aligned, prolate spheroidal coordinate system, followed by the bulk motions: 3 rotations and 3 translations in x, y and z.
- Virtual tagged images were deformed according to the model parameters and compared with the patient MR images to determine the contribution of each mode and bulk motion.^{5,6}
- A 3D mesh of material points was generated with 5 layers radially, 6 longitudinally, and 8 circumferentially. The 3D Lagrangian strain tensor, E , and fractional wall thickening, T , was calculated at each mesh point at multiple time points throughout the cardiac cycle.

MAPPING RADIATION DOSE TO THE HEART WALL

- Rigid body registration in 3D was performed to align the CT-based masks of the lung onto axial MR-based masks of the lung.
- The 3D dose field from the treatment planning system was subsampled to match the planning CT and axial MRI voxel locations.
- The dose at each material mesh point was interpolated from the nearest MRI voxels to correlate regional dose with wall mechanical strain.

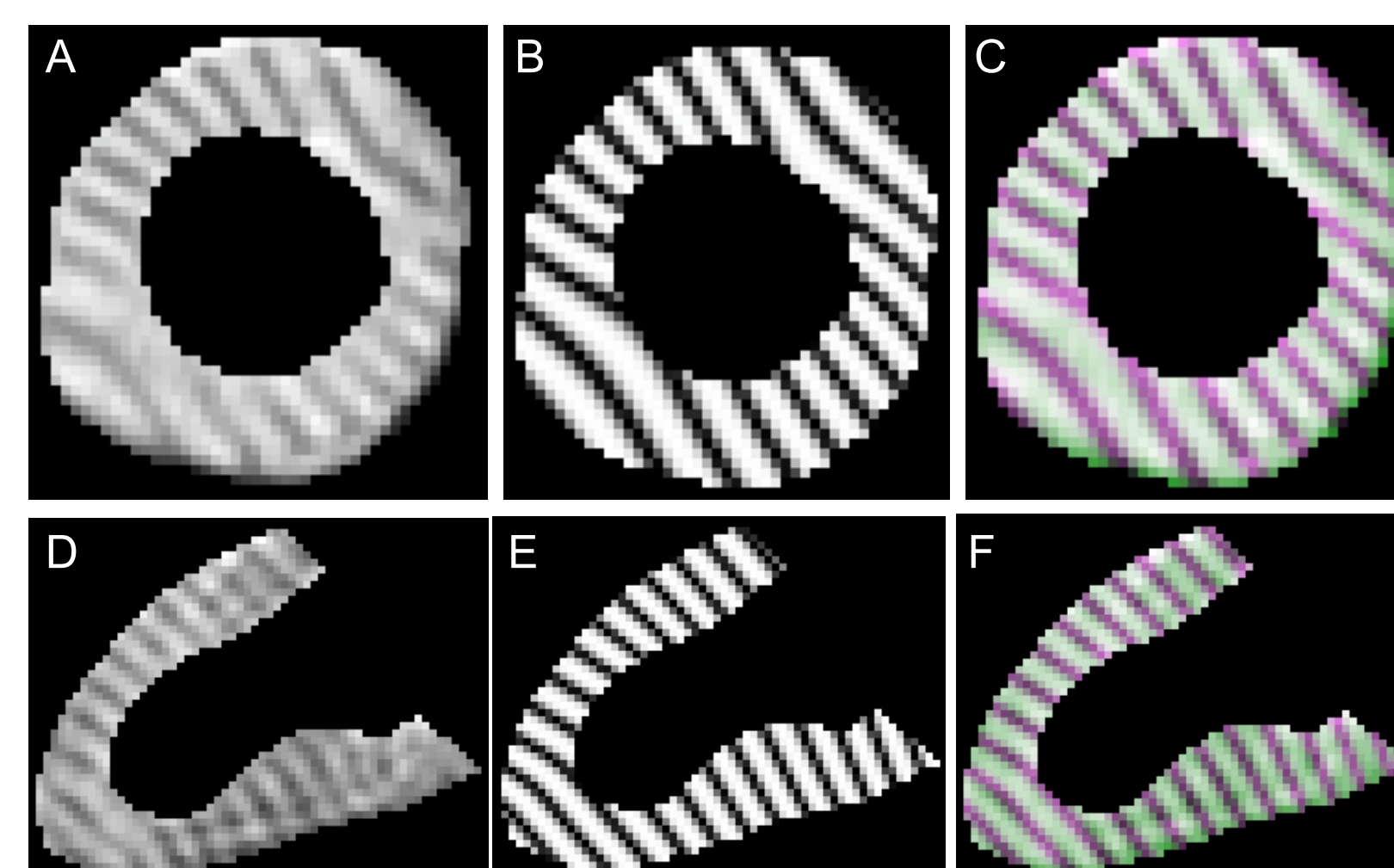
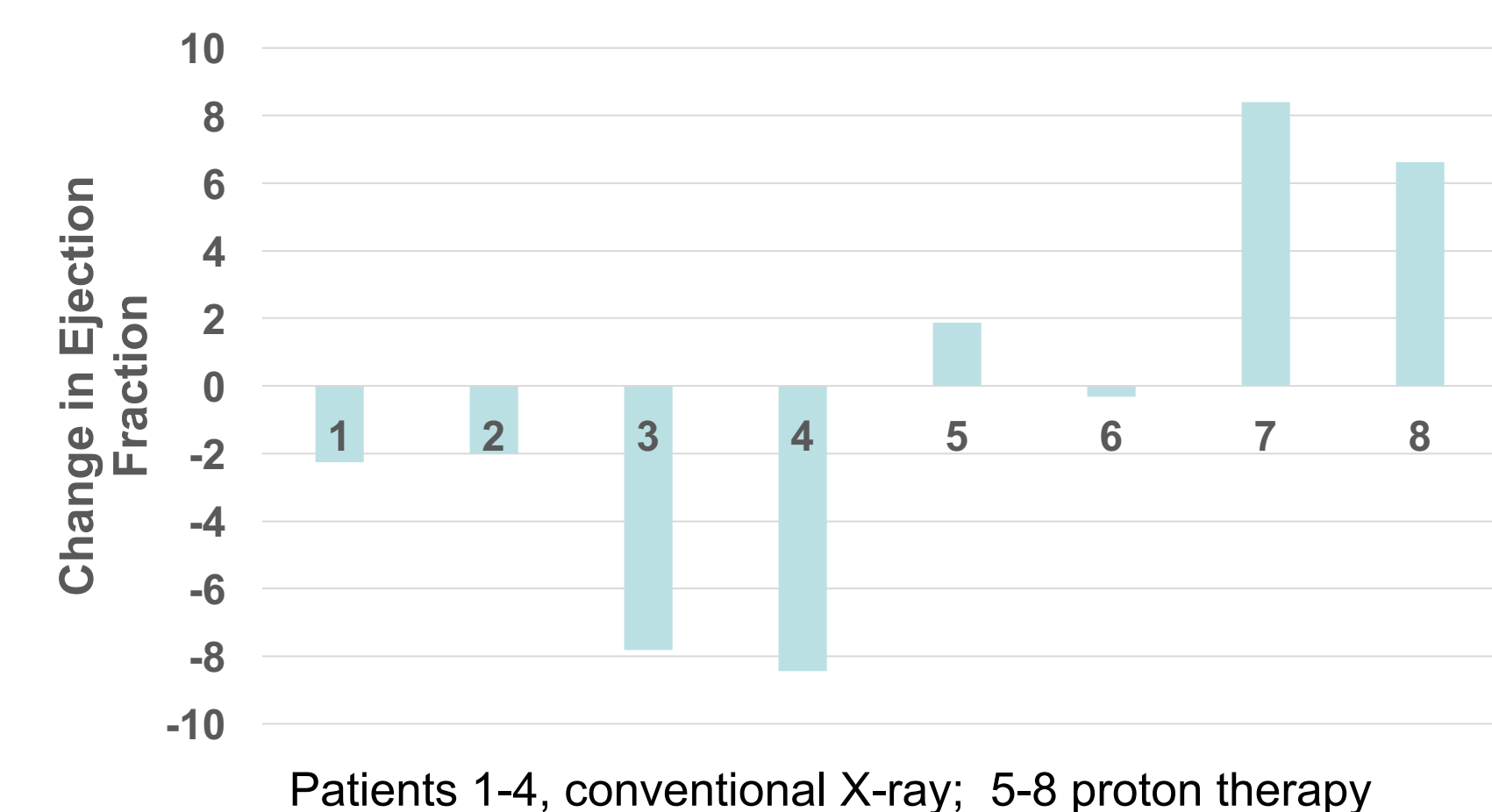


Figure 3. Modeling the deformation of parallel-tagged MR images: [A] shows a tagged short-axis MR image at end-systole after applying a cropping to the segmented endo- and epi-cardial contours. [B] shows the deformed virtual tagged image at the same slice location and time. [C] shows a color overlay where green highlights the tags in the patient MR image, pink tags in the virtual image, and darker pink results when they are well-aligned.

III. RESULTS

LEFT VENTRICULAR VOLUME AND EJECTION FRACTION:



- Data sets from 4 conventional and 4 proton therapy patients were contoured at end-diastole and end-systole by an investigator blinded to the treatment modality.
- The mean left ventricular ejection fraction (LVEF) for the 4 conventional RT patients (#1-4) was 60% before treatment and 54.87% after treatment.
- For the 4 PT patients (#5-8), the mean LVEF was 57.54% before treatment and 61.68% after treatment.
- The difference in mean change in LVEF for conventional RT (-5.13%) and proton therapy (+4.15%) patients was significantly different ($p < 0.05$).

LEFT VENTRICULAR WALL MECHANICAL STRAIN:

- Regional wall strain was computed at pre-treatment and 12-months post-treatment in a conventional RT patient.
- A statistically significant decrease in magnitude of both mean circumferential and thickening strains at end-systole were found ($p < 0.05$) post-RT compared with pre-RT.

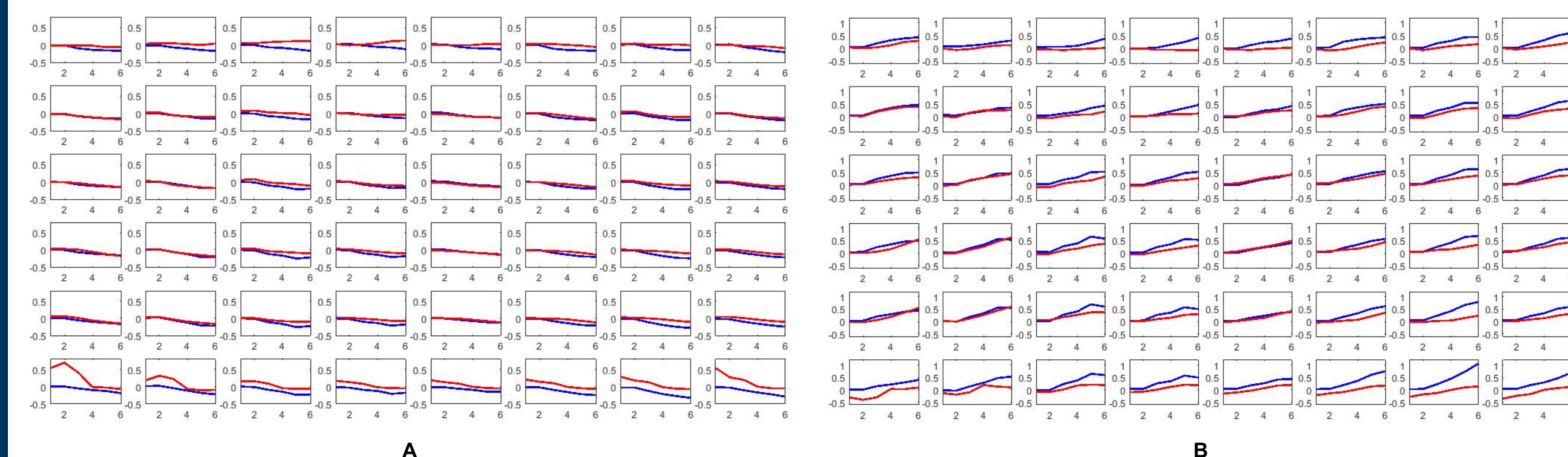


Figure 4. Circumferential strain and wall thickness multi-plots: The multi-plots in [A] and [B] show strain computed at 8 circumferential (columns) and 6 longitudinal (rows) locations around the heart left ventricle. The circumferential position starts at the mid-septum (first column) and wrapping to the free wall (4th-5th columns) and back (8th column). The longitudinal level in the heart, from base to apex, varies from the top row to the bottom row. Each mini-plot shows strain on the vertical axis as a function of time on the horizontal axis, from end-diastole to end-systole. Only radial-mid-wall strains are shown. The multi-plot in [A] presents the evolution of circumferential strain, where more negative values indicate stronger contraction. [B] presents the evolution of wall thickening strain where more positive values indicate stronger contraction. The blue curves are for the pre-RT heart, and the red curves the post-RT heart.

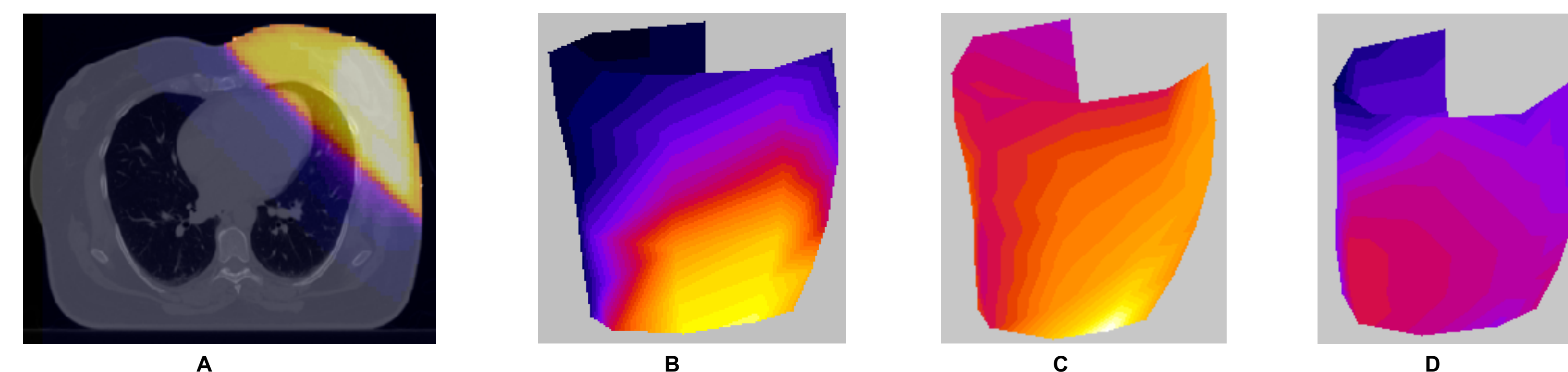


Figure 5. Heart dose calculation : [A] shows the radiation dose on a planning CT image showing elevated exposure to the anterolateral left ventricular wall and apex. [B] shows the dose distribution overlaid onto the 3D mesh of mid-wall material points. The yellow region indicates high radiation exposure while black indicates low exposure (range 2 to 47 Gy). [C] and [D] show mid-wall thickening strain at pre-RT and post-RT, respectively, with color scaled from 0 (black) to 1.0 (white). This is the color 3D rendering of the data of Figure 4B. Thickening strain is diminished over the entire heart, with larger apparent decrease in the regions with higher dose.

III. CONCLUSIONS & DISCUSSION

- A significant decrease in LVEF at 6 to 12 months post-RT was found in patients receiving conventional X-ray therapy compared with proton therapy.
- A significant decrease in heart wall circumferential and thickening strains was found post-RT in a patient receiving conventional X-ray therapy.
- These analysis techniques and initial findings are hoped to motivate and precipitate the pursuit of key clinical questions such as:
 - Does proton therapy improve the therapeutic ratio of breast cancer radiation treatment via reducing the severity of radiation toxicity to the heart?
 - Is there a role for cardiac imaging in routine clinical follow-up care of breast cancer patients for management of cardiac toxicity?
 - Can we identify breast cancer survivors that are at an elevated risk for cardiac disease who may benefit from proton therapy or altered RT?

IV. REFERENCES

- Overgaard M, Hansen PS, et al. Postoperative radiotherapy in high-risk premenopausal women with breast cancer who receive adjuvant chemotherapy. Danish Breast Cancer Cooperative Group 82b Trial. *N Engl J Med* 1997; 337: 949-55
- Darby SC, Ewertz M, et al. Risk of ischemic heart disease in women after radiotherapy for breast cancer. *N Engl J Med* 2013; 368: 987-98
- C.R. Correa et. al. Coronary artery findings after left-sided compared with right-sided radiation treatment for early-stage breast cancer. *J ClinOncol*, 25 (2007), pp. 3031-3037
- O'Dell WG, Siva Kumar S, Determining prolate spheroidal modes of cardiac deformation directly from tagged heart images, 25th ISMRM Scientific Meeting and Exhibition, Honolulu, Hawaii, [#6447] April 2017.
- C. C. Moore et al., "Three-dimensional systolic strain patterns in the normal human left ventricle: characterization with tagged MR imaging," *Radiology* 214(2), 453-466 (2000)

ACKNOWLEDGEMENTS

Funding for this work is from the Ocala Royal Dames Foundation for Cancer Research, University Scholars Program and the UF Foundation.